Supporting Information

Assignment of Infrared-active Combination Bands in the Vibrational Spectra of Protonated Molecular Clusters Using Driven Classical Trajectories: Application to N_4H^+ and N_4D^+

Reagan Hooper, Dalton Boutwell, and Martina Kaledin*

Department of Chemistry & Biochemistry, Kennesaw State University, 370 Paulding Ave NW, Box # 1203, Kennesaw, GA 30144

This document contains a table of dissociation energies and Ar binding energies (**Table 1S**), the structural parameters, harmonic vibrational frequencies of N_4H^+ and N_4D^+ with and without argon calculated at the MP2 and CCSD(T) levels of theory with aug-cc-pVDZ (AVDZ) and aug-cc-pVTZ (AVTZ) basis sets (**Tables 2S-5S**). We also found a T-shaped transition state **(Table 6S)** and predicted an N_2 rotational barrier. The electrostatic potential maps for N_4H^+ (linear minimum structure and T-shaped transition state) and N_4H^+.Ar are shown on **Figure 1S**. The symmetric internal coordinates were collected along the DMD trajectories, visualized (**Figures 2S-6S**), and the mode assignment made.

Corresponding Author

*Email: mkaledin@kennesaw.edu (M.K.)

Table S1: $N_4H^+ \rightarrow N_2H^+ + N_2$ Dissociation Energies (D_e), Zero Point Energy Corrected Values (D_0), and Binding Energies (BE) of Argon to N_4H^+ (in cm^{-1}). The Corresponding Basis Set Superposition Error[1, 2] (BSSE) Corrected Values are in Parentheses.

Method	D_e	D_0	BE (BSSE)
MP2/AVDZ	6635	6771	877 (709)
MP2/AVTZ	6530	6762	958 (838)
CCSD(T)/AVDZ	6227	6445	780 (595)
CCSD(T)/AVTZ	6138	6498	836 (720)

Table S2: Interatomic Distances R (in Å) and Harmonic Vibrational Frequencies (in cm^{-1}) of N_4H^+. ($D_{\infty h}$ symmetry). The frequency labels (ν_i) correspond to the experimental work[3].

N_4H^+	MP2 AVDZ	MP2 AVTZ	CCSD(T) AVDZ	CCSD(T) AVTZ
R(N–N)	1.1278	1.1113	1.1167	1.1010
R(N–H)	1.2791	1.2746	1.2822	1.2820
ν_1 (σ_g)	2217	2247	2380	2405
ν_3 (σ_u)	2183	2212	2345	2366
ν_6 (π_u)	1191	1227	1198	1235
ν_4 (σ_u)	602	478	376	166
ν_2 (σ_g)	434	437	434	439
ν_5 (π_g)	236	258	241	265
ν_7 (π_u)	133	138	136	143

Table S3: Interatomic Distances R (in Å) and Harmonic Vibrational Frequencies of N_4H^+. Ar (in cm^{-1}) (C_{2v} symmetry).

N_4H^+.Ar	MP2 AVDZ	MP2 AVTZ	CCSD(T) AVDZ	CCSD(T) AVTZ
R(N–N)	1.1278	1.1114	1.1166	1.1008
R(N–H)	1.2789	1.2732	1.2788	1.2752
R(Ar–H)	3.0131	2.9649	3.0853	3.0381
ν_1 (a_1)	2216	2246	2381	2404
ν_3 (b_2)	2182	2211	2346	2368
ν_6 (a_1)	1167	1206	1174	1218
ν_6' (b_1)	1196	1228	1201	1236
ν_4 (b_2)	598	502	396	168
ν_2 (a_1)	434	439	435	439
ν_5 (a_2)	236	258	241	265
ν_5' (b_2)	239	263	243	278
ν_7 (b_1)	134	139	138	143
ν_7' (a_1)	141	148	142	150
ν_8 (a_1)	67	70	63	65
ν_9 (b_2)	45	46	49	33

Table S4: Harmonic vibrational frequencies (in cm^{-1}) of N_4D^+.

N_4D^+	MP2 AVDZ	MP2 AVTZ	CCSD(T) AVDZ	CCSD(T) AVTZ
ν_1 (σ_g)	2217	2247	2380	2403
ν_3 (σ_u)	2182	2211	2345	2366
ν_6 (π_u)	868	896	873	902
ν_4 (σ_u)	422	352	268	117
ν_2 (σ_g)	433	438	434	439
ν_5 (π_g)	236	258	241	265
ν_7 (π_u)	130	135	134	140

Table S5: Harmonic Vibrational Frequencies of N_4D^+. Ar (in cm^{-1}).

N_4D^+.Ar	MP2 AVDZ	MP2 AVTZ	CCSD(T) AVDZ	CCSD(T) AVTZ
ν_1 (a_1)	2216	2246	2381	2404
ν_3 (b_2)	2181	2210	2346	2367
ν_6 (a_1)	850	881	855	890
ν_6' (b_1)	871	897	875	903
ν_4 (b_2)	428	361	286	123
ν_2 (a_1)	434	439	435	439
ν_5 (a_2)	236	258	241	265
ν_5' (b_2)	239	261	240	274
ν_7 (b_1)	131	136	135	140
ν_7' (a_1)	138	144	139	146
ν_8 (b_2)	45	46	49	33
ν_9 (a_1)	67	70	62	65

Table 6S. Interatomic Distances R (in Å), Rotational Energy Barrier and its Zero-Point Energy Corrected Value (in cm^{-1}), and Harmonic Vibrational Frequencies (in cm^{-1}) of the N_4H^+ T-shaped transition state (C_{2v} symmetry).

	MP2 AVDZ	MP2 AVTZ	CCSD(T) AVDZ	CCSD(T) AVTZ
R(H1-N2)	1.0614	1.0527	1.0603	1.0513
R(N2–N3)	1.1254	1.1087	1.1151	1.0990
R(H1-N4)	2.0831	2.0599	2.1064	2.0807
R(N4-N5)	1.1352	1.1176	1.1242	1.1072
Barrier height	5170	5083	4759	4741
ZPE value	5480	5411	5089	5208
b_2	-212	-204	-203	-194
b_2	106	110	105	108
b_1	131	128	130	128
a_1	135	147	133	143
b_2	654	742	647	745
b_1	716	783	704	782
a_1	2090	2119	2233	2255
a_1	2129	2161	2290	2314
a_1	3070	3085	3103	3120

Here, the effect of argon tag on the IR spectra was also studied and H^+/D^+ isotopic shifts predicted. **Table 1S** contains $N_4H^+ \rightarrow N_2H^+ + N_2$ dissociation energies and Ar binding energies. **Figure 1S** visualizes the electrostatic potential (ESP) maps for N_4H^+ and N_4H^+.Ar. The N_4H^+ linear structure shows the lowest ESP values at bond-ends and the highest ESP values around the cylindrical-bond surface. The N_4H^+ T-shaped transition state shows asymmetric electron cloud with positive values on N_2H^+ and negative values on N_2 perpendicular to the N_2H^+ axis. The ESP maps reveal that perfectly symmetric electron cloud surrounding the linear N_4H^+ complex becomes distorted due to the presence of Ar atom.

The structural parameters and harmonic frequencies are summarized in **Tables S2-S5**. All methods yield very similar N_4H^+ and N_4H^+.Ar structural parameters for N-H distance. The difference is less than 0.0075 Å, while the N-N bond distance agrees within 0.03 Å. The CCSD(T) level of theory provides the most accurate results, yet is impractical to carry out in direct MD simulations for N_4H^+.Ar complex, thus the accuracy and feasibility of the MP2, as an alternative, were evaluated.

The dipole spectra of $N_2{-}H^+{-}N_2$ and $N_2{-}H^+{-}N_2$.Ar and their deuterium isotopologues, calculated with MD on the fly at the MP2/AVDZ level of theory, are presented in **Figure 3**. The MD spectra for $N_2{-}H^+{-}N_2$ obtained using the analytical CCSD(T) level PES and DMS correlate closely with those of the direct MD-MP2/AVDZ simulations, validating the use of the lower level theory for the Ar-tagged species. The broad spectral region between 600 and 800 cm^{-1} relates to the parallel stretch vibration and a peak at 1190 cm^{-1} to the $N{-}H^+{-}N$ bending vibration. The H^+/D^+ isotopic shifts for parallel proton stretch and perpendicular bending vibrations are 200 cm^{-1} and 320 cm^{-1}, respectively.

The degenerate bending mode (ν_6, π_u) in N_4H^+ splits into two components (a_1 and b_1 symmetry labels) in N_4H^+.Ar. The MP2 MD simulations predicted this splitting to be about the same for both hydrogen and deuterium complexes, 21 and 17 cm^{-1}, respectively. Notably, the experimental measurements were interpreted such that in-plane/out-of-plane bending modes at 1051 / 1144 cm^{-1}, shift to 817 / 853 cm^{-1} , and the corresponding splitting is 93 / 36 cm^{-1}, respectively[3]. However, based on our assignment of the 950 cm^{-1} feature (1051 cm^{-1} in the experiment) as parallel proton motion, i.e. unrelated to ν_6, we propose the present MD derived result for the Ar-tag-induced ν_6 splitting to be definitive, at the MP2/AVDZ level of theory. For further evidence, the corresponding harmonic values are listed in the **Table 3S** and **Table 5S**.

The average absorbed energies and symmetric internal coordinates for N_4D^+ are shown on (**Figures 2S-5S**). Two fundamental frequencies identified in the DMD scan (**Figure 4**) at 525 cm^{-1} and 875 cm^{-1} absorbed energy rapidly up to 600 cm^{-1} and 2000 cm^{-1}, respectively. The corresponding symmetric coordinates displacements confirmed assignment to parallel H^+ stretch (ν_4) and perpendicular H^+ bending (ν_6) modes for 525 cm^{-1} and 875 cm^{-1}. The two combination bands at 700 cm^{-1} and 1100 cm^{-1} absorbed less energy with a time delays 1 ps and 3 ps, respectively. Large $N{-}H^+{-}N$ /N_2…N_2 stretch displacements (s_3-s_4) confirmed assignment of 700 cm^{-1} and 1100 cm^{-1} modes to $\nu_2+\nu_4$ and $2\nu_2+\nu_4$, respectively. Note similar trends in the internal symmetric coordinates profiles for N_4H^+ / N_4D^+ bending modes at 1225 cm^{-1} / 875 cm^{-1}(**Figure 6S**).

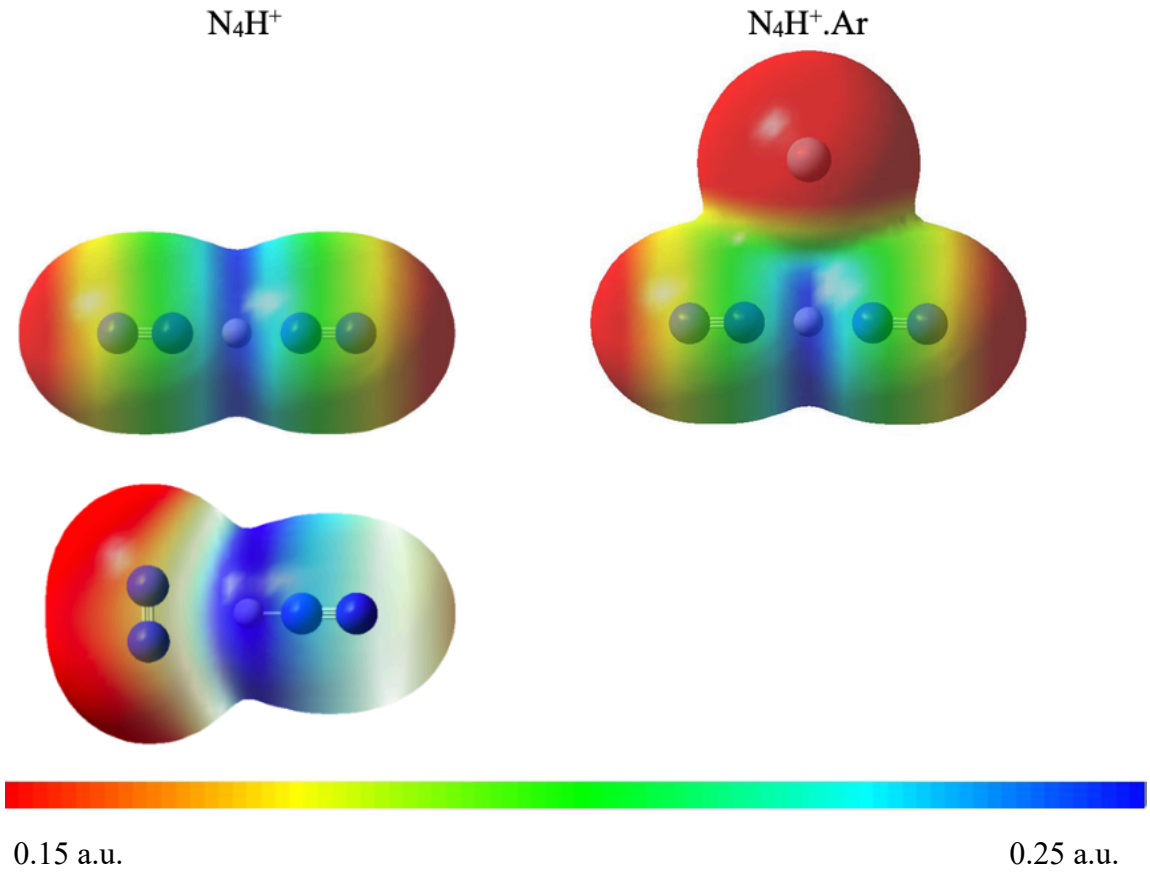

Figure 1S: Electrostatic potential maps at B3LYP/AVTZ level of theory (density isovalues=0.0004 a.u.) for N_4H^+ and N_4H^+.Ar.

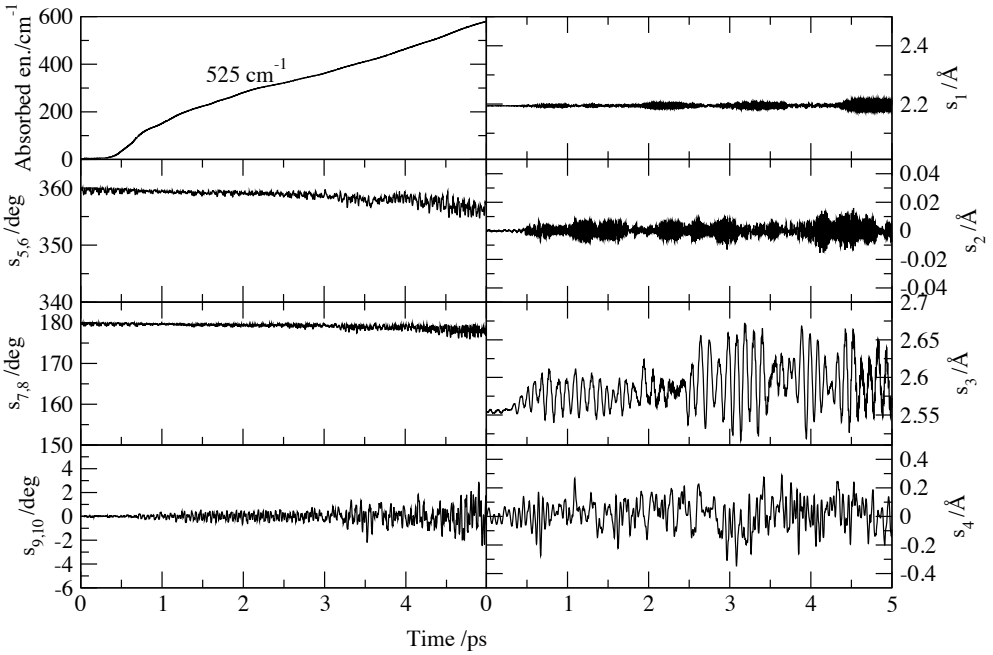

Figure 2S: Average absorbed energy (in cm^{-1}) and symmetric internal coordinates $s_{1\text{-}10}$ along the N_4D^+ DMD trajectories for ν_4=525 cm^{-1} frequency. The intensity of the electric field was 25 mV/bohr.

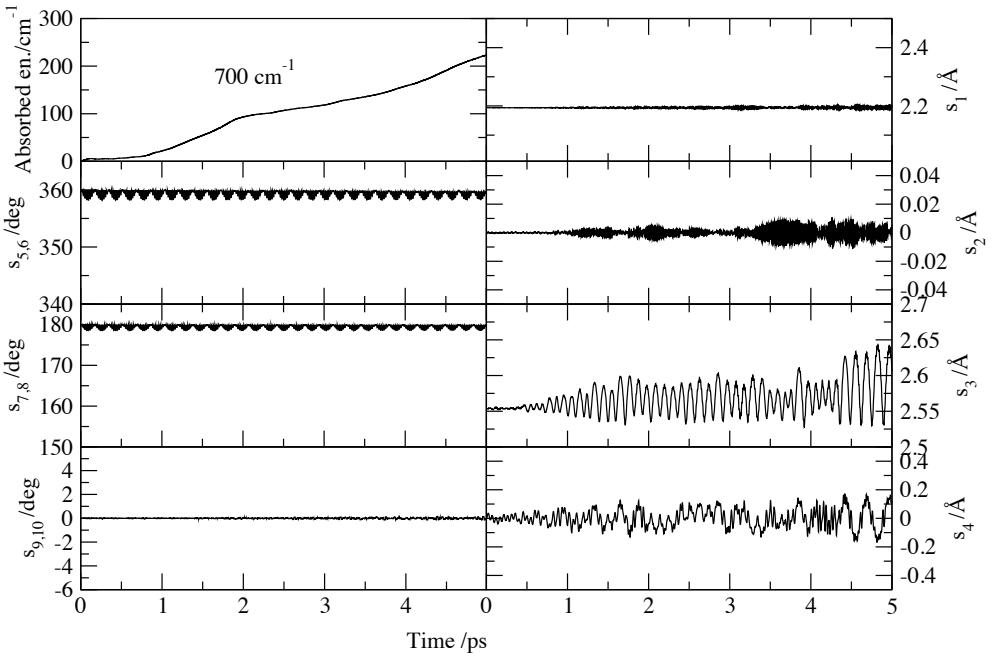

Figure 3S: Average absorbed energy (in cm^{-1}) and symmetric internal coordinates $s_{1\text{-}10}$ along the N_4D^+ DMD trajectories for $\nu_2+\nu_4$=700 cm^{-1} frequency. The intensity of the electric field was 25 mV/bohr.

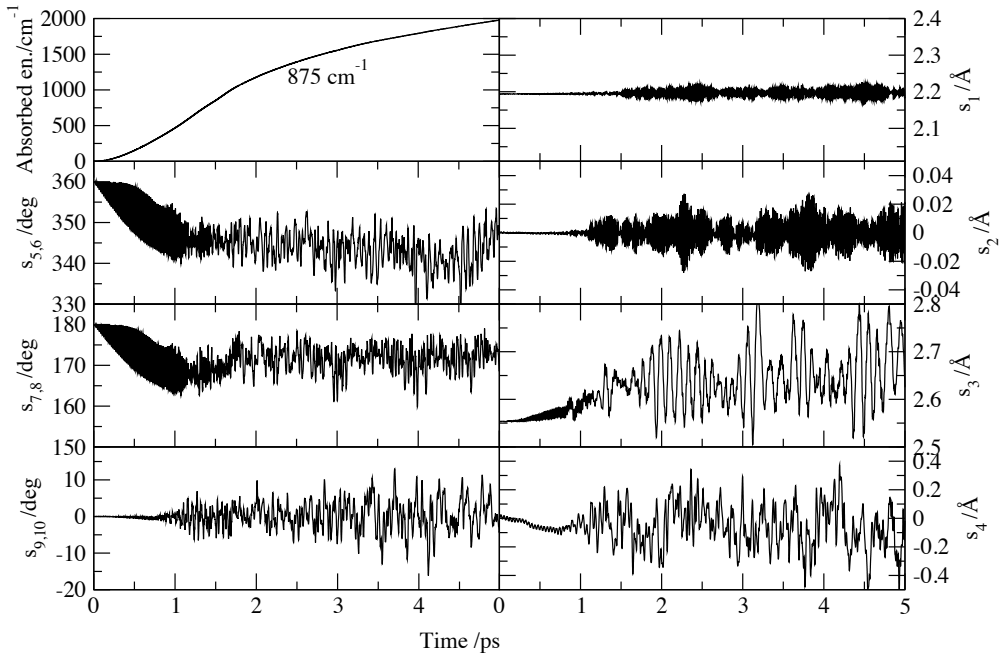

Figure 4S: Average absorbed energy (in cm^{-1}) and symmetric internal coordinates $s_{1\text{-}10}$ along the N_4D^+ DMD trajectories for ν_6=875 cm^{-1} frequency. The intensity of the electric field was 25 mV/bohr.

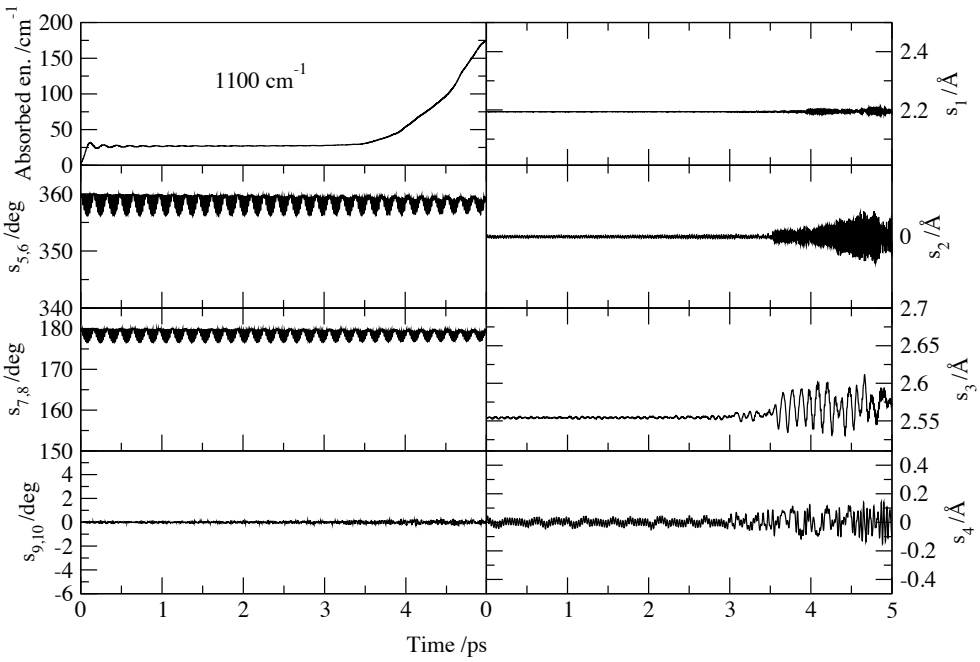

Figure 5S: Average absorbed energy (in cm^{-1}) and symmetric internal coordinates $s_{1\text{-}10}$ along the N_4D^+ DMD trajectories for $2\nu_2+\nu_4$=1100 cm^{-1} frequency. The intensity of the electric field was 75 mV/bohr.

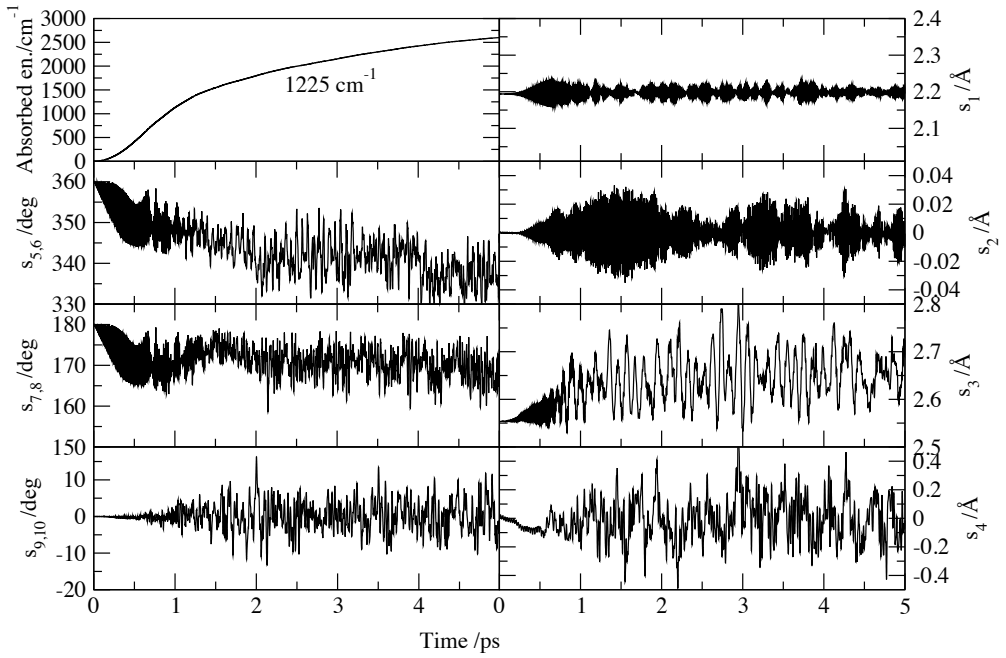

Figure 6S: Average absorbed energy (in cm^{-1}) and symmetric internal coordinates $s_{1\text{-}10}$ along the N_4H^+ DMD trajectories for ν_6=1225 cm^{-1} frequency. The intensity of the electric field was 25 mV/bohr.

References

(1) Boys, S. F.; Bernardi, F. The calculation of small molecular interactions by the differences of separate total energies. Some procedures with reduced errors. *Mol. Phys*. **1970**, *19***,** 553-566.

(2) Simon, S.; Duran, M.; Dannenberg, J. J. How does basis set superposition error change the potential surfaces for hydrogen-bonded dimers? *J. Chem. Phys*. **1996**, *105,* 11024-11031.

(3) Ricks, A. M.; Douberly, G. E.; Duncan, M. A.; Infrared Spectroscopy of the Protonated Nitrogen Dimer: The complexity of Shared Proton Vibrations. *J. Chem. Phys.* **2009**, *131*, 1045312.